

Ba(Ti_{1-x}Zr_x)O₃ relaxors: Dynamic ferroelectrics in the gigahertz frequency rangeS. Lisenkov , A. Ladera , and I. Ponomareva*Department of Physics, University of South Florida, Tampa, Florida 33620, USA* (Received 27 August 2020; revised 26 October 2020; accepted 11 December 2020; published 23 December 2020)

Relaxor ferroelectrics are of great scientific and technological significance as they exhibit large and unusual responses to external stimuli. Their hallmark features are broadness and frequency dispersion of the peak in the temperature dependence of the dielectric constant. Both are believed to originate from the dynamics of polar nanoregions. We apply first-principles-based molecular dynamics to resolve the gigahertz electric response of dynamically poled Ba(Ti_{1-x}Zr_x)O₃ ferroelectric relaxors that remained overlooked so far. We find that (i) the hallmark relaxor features continue to persist even in the dynamically poled structures, but do not necessarily originate from the polar nanoregions dynamics; (ii) dynamically poled samples exhibit polarization aging which leads to the frequency dependence of both remnant polarization and the Curie temperature; (iii) “dynamical” nature of the latter naturally explains the frequency dependence of the dielectric susceptibility maximum in dynamically poled Ba(Ti_{1-x}Zr_x)O₃; and (iv) incorporation of the polarization aging into dielectric susceptibility expression explains its enhancing contribution in an intuitive way.

DOI: [10.1103/PhysRevB.102.224109](https://doi.org/10.1103/PhysRevB.102.224109)**I. INTRODUCTION**

Relaxor ferroelectrics [1–4], or relaxors, are famous for their giant dielectric permittivity and electromechanical coupling, which make them a primary material for many applications. They have been studied since 1954 [5] and are still in the spotlight [6–10]. A hallmark feature of relaxors is a broad maximum in temperature dependence of the dielectric permittivity, whose position, T_m , is shifted to lower temperatures as the frequency of the probing field decreases [1]. Unlike ferroelectrics, T_m does not correspond to a phase transition from a paraelectric to a long-range-ordered ferroelectric state with homogeneous polarization. Instead, it is presently accepted that the polarization is correlated on a local scale leading to the appearance of polar nanoregions whose behavior underlies properties of relaxors [2]. While a normal ferroelectric is characterized by well-defined Curie temperature, that is not the case for a relaxor. Several characteristic temperatures are commonly used for them. The Burns temperature T_B is associated with transformation from a paraelectric state, similar to that of regular ferroelectric, to an ergodic relaxor state which is believed to originate from the appearance of mobile polar nanoregions. On cooling, the dynamics of polar nanoregions slows down and eventually freezes giving rise to the nonergodic state in canonical relaxors at the temperature T_f . It is further believed that this freezing is the origin of the relaxor hallmark dielectric behavior, which is the broadness and characteristic dispersion of the dielectric susceptibility peak. The ferroelectric phase can be induced in the nonergodic state of the relaxor by the application of the electric field via irreversible transformation. Subsequent heating transforms the ferroelectric phase to the ergodic one at T_C . In other relaxors, the ergodic phase transitions into a ferroelectric phase upon cooling [1]. Experimentally, T_B is

the temperature at which the dielectric susceptibility starts deviating from the Curie-Weiss behavior associated with the paraelectric phase of normal ferroelectrics. T_f is typically obtained from fitting the experimental data on the frequency dispersion of T_m to the phenomenological Vogel-Fulcher law $f = f_0 e^{-E_b/(T_m - T_f)}$, where f_0 , E_b , and T_f are the fitting parameters [2], although care needs to be taken in using this expression to identify T_f [1]. It is also the temperature below which the irreversible transition into the ferroelectric phase occurs in canonical relaxors. At the same time, the connection between thus obtained empirical T_f and T_B and the polar nanoregions dynamics model is not direct, which explains why the subject of polar nanoregions is still under debate after decades of intense research [3]. The general rule is that the relaxor behavior can only be observed in disordered crystals.

Among different disordered crystal relaxors with isovalent substitution, such as Ba(Ti_{1-x}Zr_x)O₃ and Ba(Ti_{1-x}Sn_x)O₃, are fascinating, as not only do they exhibit the relaxor behavior in the absence of nominal charge disorder but also exhibit a more gradual crossover between the normal ferroelectric and relaxor state as the Zr (or Sn) concentration increases. For example, in Ba(Ti_{1-x}Zr_x)O₃ increase of Zr leads to the merging of the three phase transitions of parent BaTiO₃ at the point of the pinched phase transition, $x = 0.1$. In the concentration range $0.15 \leq x \leq 0.20$ a diffused phase transition occurs that is associated with a broad peak in the dielectric susceptibility [2]. In this region both frequency dependent and independent behavior can occur depending on whether the experimental observation rates are close to the relaxation times [2]. For $x \geq 0.25$, the frequency dependence of T_m follows the Vogel-Fulcher law typical of relaxors. Dielectric measurements for Ba(Ti_{1-x}Zr_x)O₃ in the frequency range $10^{-2} \leq f \leq 10^5$ Hz revealed frequency dispersion for T_m for $x > 0.20$ [11]. The

investigation of $\text{Ba}(\text{Ti}_{0.675}\text{Zr}_{0.325})\text{O}_3$ in the same frequency range [12] reported that its scaling characteristics differ from those in classical complex perovskite relaxors, suggesting a different origin of dielectric relaxation.

However, the majority of the studies focus on the frequency range below 10 MHz [3] and unpoled samples. The former one limits resolving dynamics that originates from the relaxation times smaller than 10^{-7} s, while the latter overlooks the polarization relaxation and aging. In addition, the higher frequency range bridges the polar nanoregions dynamics with the one that originates from the phonon contribution [9] which could potentially lead to unusual behavior. In Ref. [9] the complex dielectric response of $\text{Ba}(\text{Zr}_{0.5}\text{Ti}_{0.5})\text{O}_3$ was investigated using molecular dynamics (MD) simulations in the frequency range of 1 GHz to 1 THz and the temperature range of 5–1000 K to predict that the relaxation-type polarization processes dominate in the dielectric response of disordered $\text{Ba}(\text{Zr}_{0.5}\text{Ti}_{0.5})\text{O}_3$ for all temperatures in contrast with lead-based perovskite relaxors in which the response is purely of phonon nature for $T > T_B$ and the relaxation only appears below T_B . Experimentally $\text{Ba}(\text{Zr}_{0.25}\text{Ti}_{0.75})\text{O}_3$ dielectric response was measured at 1 MHz to 3 GHz in the temperature range -50 – 100 °C [13]. Dielectric relaxation was observed in the whole frequency range even above T_m . The relaxation frequency ranged from 10^8 to 10^{12} Hz for the temperature range -50 – 80 °C [13]. Application of broadband dielectric spectroscopy from Hz up to the infrared range and temperature interval 10–300 K to $\text{Ba}(\text{Ti}_{1-x}, \text{Zr}_x)\text{O}_3$ with $x = 0.6, 0.7,$ and 0.8 suggested that $\text{Ba}(\text{Ti}_{1-x}, \text{Zr}_x)\text{O}_3$ is to be considered as a dipolar glass rather than a relaxor ferroelectric [14].

There is, however, one aspect of the dynamics that remains mostly unknown. It is the relaxors response to the dynamical poling. The dynamical poling can be achieved by application of the ac electric field whose frequency approaches the characteristic frequencies of the material. Unlike normal ferroelectrics, relaxors exhibit aging so dynamical poling can shed some unique light into their dynamics. Poled relaxors are also the primary candidates for piezoelectric devices [3]. The aims of this work are to (i) fill this gap and provide an atomistic insight into the high frequency electric response of dynamically poled $\text{Ba}(\text{Ti}_{1-x}, \text{Zr}_x)\text{O}_3$; (ii) reveal how the dynamics of $\text{Ba}(\text{Ti}_{1-x}, \text{Zr}_x)\text{O}_3$ evolve with composition, that is, across the ferroelectric-to-relaxor transition; (iii) predict that the dynamically poled $\text{Ba}(\text{Ti}_{1-x}, \text{Zr}_x)\text{O}_3$ exhibit the hallmark features of relaxors at gigahertz; and (iv) elucidate the origin of these features in dynamically poled relaxors.

II. METHODOLOGY

To achieve our aims we turn to atomistic MD simulations based on the effective Hamiltonian that we previously derived for $\text{Ba}(\text{Ti}_{1-x}, \text{Zr}_x)\text{O}_3$ from first principles [15]. The degrees of freedom for the Hamiltonian include local soft modes which are proportional to the local dipole moments and local strain variables that describe deformation of the unit cells. The Hamiltonian includes the interactions that are responsible for the ferroelectricity, such as local mode self-energy up to fourth order, harmonic short- and long-range interactions between the local modes, elastic deformations, and interactions responsible for the electrostriction [16]. The effective Hamil-

tonian accurately reproduces the complex phase diagram of $\text{Ba}(\text{Ti}_{1-x}, \text{Zr}_x)\text{O}_3$ in a very wide compositional and temperature range including such subtle features as the pinched phase transition point and the temperature dependence of the peak in the dielectric susceptibility [15]. The bulk sample is simulated by a supercell of $30 \times 30 \times 30$ unit cells of BaTiO_3 , with Zr ions placed randomly to model the desired Zr concentration. Technically, we considered $x = 0.00, 0.14, 0.16, 0.18, 0.20, 0.30, 0.40,$ and 0.50 . Periodic boundary conditions are applied along all three Cartesian directions to model the bulk sample. We simulated an *NPT* ensemble (constant number of particles, pressure, and temperature) with temperature controlled by the Evans-Hoover thermostat [17] which preserves kinetic energy at each MD step. It should be noted that in principle the thermostat can affect the dynamics of the system as it introduces a fictitious force into the equation of motion. However, this particular one was previously found to produce accurate dynamical predictions within similar computational framework [18–20]. The temperature range was 250–400 K for $\text{Ba}(\text{Ti}_{1-x}, \text{Zr}_x)\text{O}_3$ and 270–550 K for BaTiO_3 . An electric ac field was simulated by adding the $-\mathbf{P} \cdot \mathbf{E}(t)$ term to the effective Hamiltonian, where \mathbf{P} and \mathbf{E} are the polarization and electric field, respectively. We simulated frequencies in the range 0.5–5.0 GHz with the step of 0.5 GHz. The frequency range was chosen to fit at its lower end within our computational capabilities and at the upper end not to overlap with the polar mode frequency of cubic BaTiO_3 . For each frequency we carried out simulations for three different directions of the electric field: [100], [110], and [111] in pseudocubic axes. The amplitude of the electric field was 1500 kV/cm. It should be noted that while the amplitude of the field may appear large the actual findings will be limited to the experimentally accessible fields. Any field amplitude larger than the coercive field is expected to result in the same behavior. Consequently, setting the amplitude large in simulations is an efficient strategy when the coercive fields are not known beforehand. In each case we simulate ten periods of the electric field and then average the data. The averages over the ten periods are reported.

III. RESULTS AND DISCUSSION

We begin by analyzing computational data for the [100] electric field. Figure 1 shows representative hysteresis loops for BaTiO_3 and $\text{Ba}(\text{Ti}_{1-x}, \text{Zr}_x)\text{O}_3$ with different Zr concentrations computed at 270 K. We also included experimental data from the literature to test the accuracy of our predictions. Following are the findings from the data. Firstly, in all instances the coercive field decreases with the frequency as was established for the intrinsic polarization reversal [21]. Secondly, the zero-field slope in $P(E)$, or the dielectric susceptibility, χ , is independent of frequency for BaTiO_3 but exhibits frequency dependence for $\text{Ba}(\text{Ti}_{1-x}, \text{Zr}_x)\text{O}_3$. Thirdly, the zero-field polarization, P_r^* in BaTiO_3 , is independent of the frequency, while for $\text{Ba}(\text{Ti}_{1-x}, \text{Zr}_x)\text{O}_3$ it is frequency dependent. Note the use of the star to distinguish from the usual frequency independent remnant polarization. To quantify the latter two features we plot the zero field χ and P_r^* as a function of temperature for different Zr concentrations in Fig. 2. To obtain both quantities $P(E)$ loops were fitted with a polynomial up to

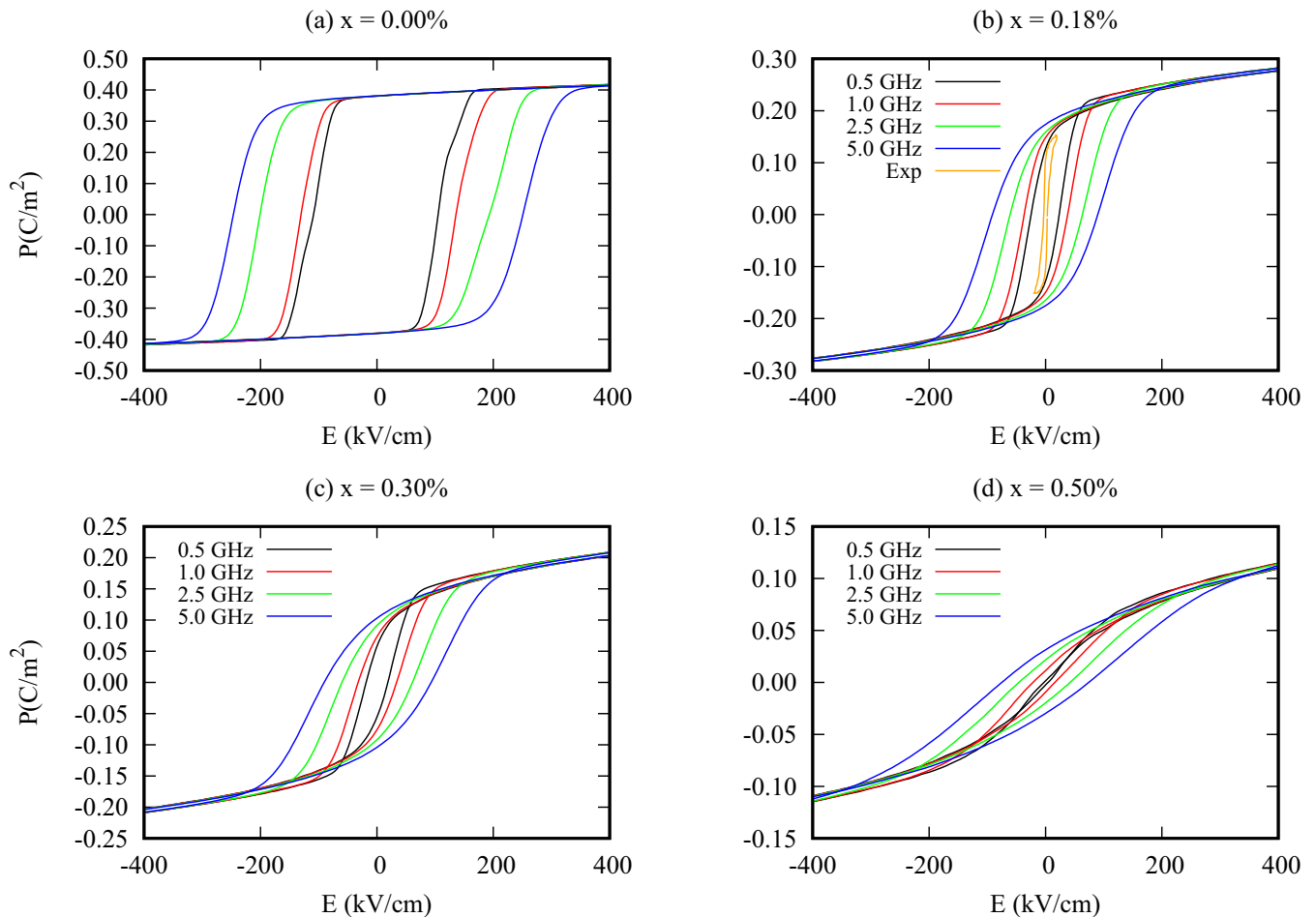


FIG. 1. Polarization as a function of electric field computed for different frequencies at 270 K. Different panels correspond to different x as given in the titles. Experimental data (Exp) are for 220 K and are taken from Ref. [8].

third order in the vicinity of $E = 0$. The zeroth- and first-order terms were used to obtain P_r^* and χ , respectively. Note that we added experimental data from the literature for both χ and P to test the accuracy of our predictions.

The temperature evolution of χ [Figs. 2(a)–2(c)] offers a surprising finding: the two hallmark features of relaxors—the broadness of the dielectric response and the frequency dispersion of its maximum—persist under gigahertz dynamical poling. Another unexpected finding is the frequency dispersion for the T_m of BaTiO₃ in the same frequency range. The latter finding suggests that in BaTiO₃ there exists intrinsic relaxation already in gigahertz, and that it is capable of producing a frequency dispersion similar to the one typically attributed to the polar nanoregions dynamics in relaxors. This intrinsic relaxation could be due to the central mode associated with hopping of the off-centered Ti ions as discussed in Ref. [22]. In the same work it was stated that the central mode excitation with frequencies below the phonon response appears in pure BaTiO₃. The prediction of the T_m dispersion at gigahertz in BaTiO₃ implies that the polar nanoregions dynamics is not the only mechanism that could lead to the observed behavior since such polar nanoregions are not expected in homogeneous materials.

Figures 2(d)–2(f) reveal that in Ba(Ti_{1-x}Zr_x)O₃ P_r^* exhibits frequency dependence in the entire temperature range

investigated. At the intuitive level lower frequency allows the system to relax and lose P_r^* , which can be understood as “ferroelectric” relaxation, or aging. On the other hand, for BaTiO₃ the dependence is limited to the vicinity of the Curie point. This could be explained by either drastic softening of the ferroelectric soft mode on approaching the Curie point in the paraelectric phase, which increases intrinsic relaxation time or by the central mode [22]. To quantify the effect of aging at 270 K we plot normalized P_r^* as a function of inverse frequency in Fig. 3. The data demonstrates the presence of aging in Ba(Ti_{1-x}Zr_x)O₃ but not in BaTiO₃. The frequency dependence of P_r^* leads to an important consequence, namely, that the temperature associated with the onset of P_r^* , is also frequency dependent which is evident from Figs. 2(d)–2(f). Therefore, in this case we actually have a “dynamic” Curie temperature, T_C^* , whose frequency dependence is given in Figs. 2(g)–2(i). From the figure we see that in the frequency range of 0.5–5 GHz the dynamic Curie temperature varies by 50, 80, and 100 K for $x = 0.00$, 0.18, and 0.30, respectively. In all cases T_C^* increases with the frequency. In normal ferroelectrics, T_m and T_C coincide. To explore this relationship for the dynamic Curie temperature we added computational T_m to Figs. 2(g)–2(i). The data reveal a strong correlation between T_m and T_C^* which predicts that the frequency dispersion of T_m in this case originates from the frequency dependence

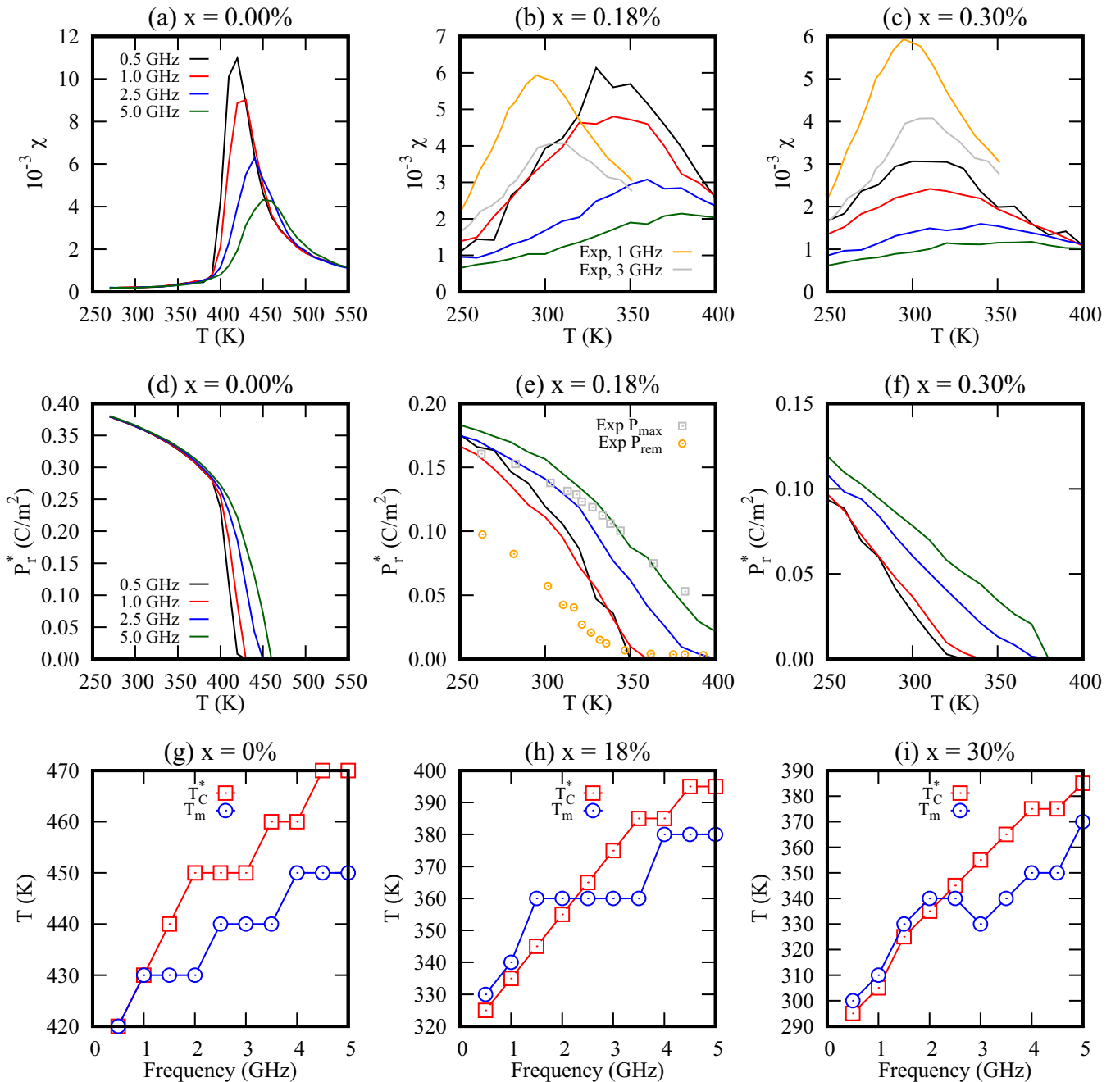


FIG. 2. The temperature evolution of the zero-field dielectric susceptibility (a)–(c) and dynamic remnant polarization (d)–(f). Frequency dependence of T_C^* and T_m (g)–(i). Zr concentrations are given in the titles. Experimental data (Exp) for the maximum, P_{\max} , and remnant, P_r , polarization are for $x = 0.15$ and taken from Ref. [8]. Experimental data (Exp) for $\chi(T)$ are for $x = 0.25$ and taken from [13].

of the dynamic Curie temperature. Our findings suggest that in the given frequency range $\text{Ba}(\text{Ti}_{1-x}\text{Zr}_x)\text{O}_3$ behaves like a dynamic ferroelectric exhibiting different ferroelectric properties (P_r^* , T_C^* , and χ) at different frequencies, while still fulfilling the relationship between them common to ferroelectrics.

Another feature displayed in Figs. 2(a)–2(c) is the broadness of the susceptibility peak in the entire frequency range. A comparison of P_r^* for BaTiO_3 and $\text{Ba}(\text{Ti}_{1-x}\text{Zr}_x)\text{O}_3$ [Figs. 2(d)–2(f)] demonstrates the difference in the temperature evolution of P_r^* : for BaTiO_3 it

is first-order-like in nature and for $\text{Ba}(\text{Ti}_{1-x}\text{Zr}_x)\text{O}_3$ it is second-order-like. The second-order phase transitions are mostly of order-disorder type. In our case, the introduction of ferroelectrically inactive Zr in BaTiO_3 disrupts ionic arrangement associated with the soft ferroelectric mode, thus creating more disordered dipole configurations that are likely to favor order-disorder transition. The second-order character of the diffused phase transition was also reported in the experimental study of Ref. [22]. We have repeated all simulations and data analysis for the other two directions of the applied electric field and found similar behavior and

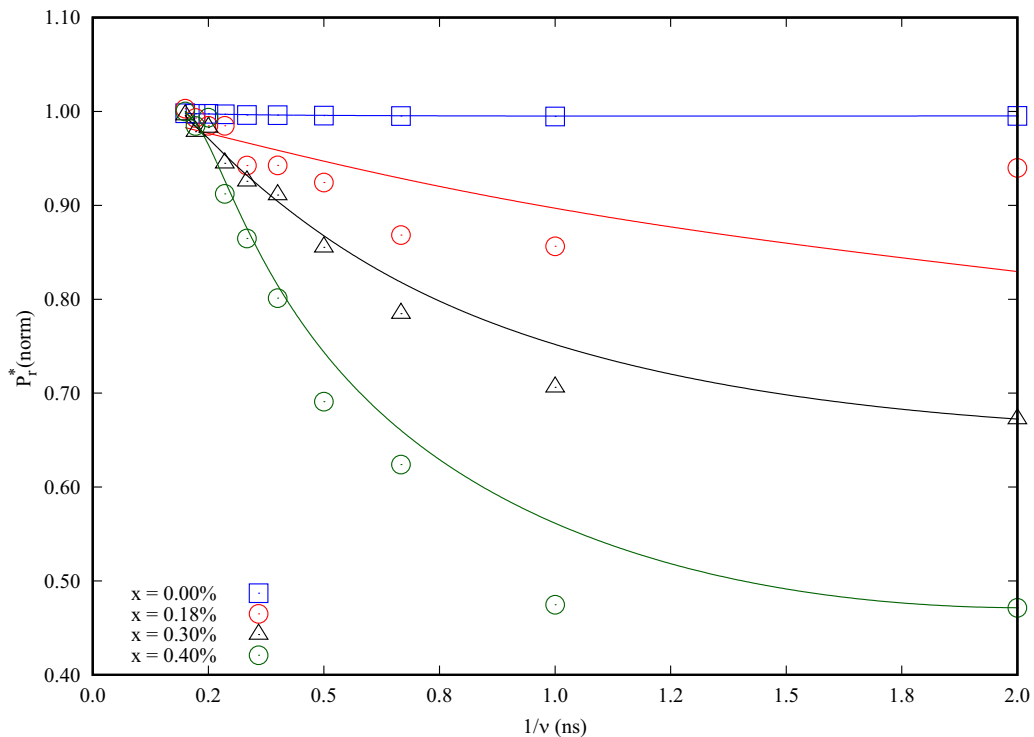


FIG. 3. Normalized dynamic remnant polarization as a function of inverse frequency at 270 K.

trends, allowing for extending our conclusions to other field directions.

It is interesting to see whether ferroelectric relaxation contributes to zero-field susceptibility. We can formally write $dP = (\frac{\partial P}{\partial E})_t dE + (\frac{\partial P}{\partial t})_E dt = [(\frac{\partial P}{\partial E})_t + (\frac{\partial P}{\partial t})_E \frac{1}{\partial E / \partial t}] dE$ which gives zero-field susceptibility $\chi = \frac{dP}{dE} = (\frac{\partial P}{\partial E})_t + (\frac{\partial P}{\partial t})_{E=0} \frac{1}{\partial E / \partial t}$ and suggests that the polarization relaxation makes a contribution to the dielectric susceptibility. In the case of the ac field the polarization relaxation, $(\frac{\partial P}{\partial t})_{E=0}$, and the rate of field application, $\partial E / \partial t$, have the same sign so that the relaxation term enhances the susceptibility. This is readily seen from inspection of the zero-field regions in Figs. 1(a) and 1(b). In the case of Ba(Ti_{1-x}Zr_x)O₃ the ferroelectric relaxation clearly enhances the slope on going from the largest to the lowest frequencies. Furthermore, we can approximate $(\frac{\partial P}{\partial t})_{E=0} \approx \frac{P_r}{\tau}$, where τ is the relaxation time. The approximation suggests that the relaxation term makes a stronger contribution when the relaxation time is short like in relaxors. On the other hand, in normal ferroelectrics away from the Curie temperature τ is nearly infinity so the term stops contributing. The term also is not expected to contribute strongly when $P_r = 0$ as in dielectrics or in the paraelectric phase.

What could be the imprint of the polarization relaxation dynamics in relaxor properties outside the dynamic poling setting? Firstly, one can speculate that the same mechanism takes place at lower frequencies and field amplitudes. Indeed, due to the presence of aging the sample will appear nonpolar in all static or very low frequency measurements. At the same time it may experience dynamical poling under the measurement conditions and therefore exhibit the relaxational dynamics resolved in simulations. Secondly, individual polar nanoregions could experience dynamical poling

and thus provide the associated contribution to the dielectric response.

IV. CONCLUSIONS

In summary, we have used first-principles-based MD simulations to investigate gigahertz electric response of dynamically poled Ba(Ti_{1-x}Zr_x)O₃ in a wide compositional range. Simulations predict strong aging effects in Ba(Ti_{1-x}Zr_x)O₃ in the temperature range 250–400 K. Some aging also occurs in BaTiO₃ in the vicinity of Curie temperature. This aging leads to the concept of dynamical polarization and Curie temperature which exhibit frequency dependence. In particular T_C^* increases with the frequency in the range 0.5–5 GHz. This increase is closely followed by the peak in the dielectric susceptibility and thus leads to the frequency dispersion for T_m . This frequency dispersion of T_m mirrors the hallmark relaxor feature, although it is likely to originate from the intrinsic relaxation rather than polar nanoregion dynamics. The other hallmark feature, namely, the broadness of the dielectric response peak, is also present in dynamically poled Ba(Ti_{1-x}Zr_x)O₃ and is traced to the second-order behavior of the order parameter, the dynamical polarization. Our findings advance the present understanding of relaxor dynamics by providing predictions in the domain of dynamical poling that has not been explored thus far.

ACKNOWLEDGMENTS

The present work is supported by the U.S. Department of Energy, Office of Basic Energy Sciences, Division of Materials Sciences and Engineering under Grant No. DE-SC0005245.

- [1] A. Bokov and Z. G. Ye, *J. Mater. Sci.* **41**, 31 (2006).
- [2] V. V. Shvartsman and D. C. Lupascu, *J. Am. Ceram. Soc.* **95**, 1 (2012).
- [3] F. Li, S. Zhang, D. Damjanovic, L.-Q. Chen, and T. R. Shrout, *Adv. Funct. Mater.* **28**, 1801504 (2018).
- [4] A. A. Bokov and Z.-G. Ye, *J. Adv. Dielectr.* **02**, 1241010 (2012).
- [5] G. Smolenskii and V. Isupov, *Zh. Tekh. Fiz.* **24**, 1375 (1954).
- [6] H. Takenaka, I. Grinberg, S. Liu, and A. M. Rappe, *Nature (London)* **546**, 391 (2017).
- [7] Z. Kutnjak, J. Petzelt, and R. Blinc, *Nature (London)* **441**, 956 (2006).
- [8] A. Pramanick, W. Dmowski, T. Egami, A. S. Budisuharto, F. Weyland, N. Novak, A. D. Christianson, J. M. Borreguero, D. L. Abernathy, and M. R. V. Jørgensen, *Phys. Rev. Lett.* **120**, 207603 (2018).
- [9] D. Wang, A. Bokov, Z.-G. Ye, J. Hlinka, and L. Bellaiche, *Nat. Commun.* **7**, 11014 (2016).
- [10] Q. Chaorui, B. Wang, N. Zhang, S. Zhang, J. Liu, D. Walker, Y. Wang, H. Tian, T. Shrout, Z. Xu, L.-Q. Chen, and F. Li, *Nature (London)* **577**, 350 (2020).
- [11] V. V. Shvartsman, J. Zhai, and W. Kleemann, *Ferroelectrics* **379**, 77 (2009).
- [12] A. A. Bokov, M. Maglione, A. Simon, and Z. G. Ye, *Ferroelectrics* **337**, 169 (2006).
- [13] J. Li, H. Kakemoto, S. Wada, T. Tsurumi, and H. Kawaji, *J. Appl. Phys.* **100**, 024106 (2006).
- [14] J. Petzelt, D. Nuzhnyy, M. Savinov, V. Bovtun, M. Kempa, T. Ostapchuk, J. Hlinka, G. Canu, and V. Buscaglia, *Ferroelectrics* **469**, 14 (2014).
- [15] C. Mentzer, S. Lisenkov, Z. G. Fthenakis, and I. Ponomareva, *Phys. Rev. B* **99**, 064111 (2019).
- [16] W. Zhong, D. Vanderbilt, and K. M. Rabe, *Phys. Rev. B* **52**, 6301 (1995).
- [17] D. Rapaport, *The Art of Molecular Dynamics Simulation* (Cambridge University Press, Cambridge, UK, 1997).
- [18] B. K. Mani, C.-M. Chang, and I. Ponomareva, *Phys. Rev. B* **88**, 064306 (2013).
- [19] Z. G. Fthenakis and I. Ponomareva, *Phys. Rev. B* **96**, 184110 (2017).
- [20] C.-M. Chang, B. K. Mani, S. Lisenkov, and I. Ponomareva, *Ferroelectrics* **494**, 68 (2016).
- [21] M. Kingsland, Z. G. Fthenakis, and I. Ponomareva, *Phys. Rev. B* **100**, 024114 (2019).
- [22] D. Nuzhnyy, J. Petzelt, M. Savinov, T. Ostapchuk, V. Bovtun, M. Kempa, J. Hlinka, V. Buscaglia, M. T. Buscaglia, and P. Nanni, *Phys. Rev. B* **86**, 014106 (2012).